A poxvirus protein forms a complex with left-handed Z-DNA: Crystal structure of a Yatapoxvirus Zα bound to DNA

Sung Chul Ha*, Neratur K. Lokanath*, Dong Van Quyen*, Chun Ai Wu*, Ky Lowenhaupt†, Alexander Rich†‡, Yang-Gyun Kim‡§, and Kyeong Kyu Kim*‡

*Department of Molecular Cell Biology, Samsung Biomedical Research Institute, Sungkyunkwan University School of Medicine, Suwon 440-746, Korea; †Department of Biology, Massachusetts Institute of Technology, Cambridge, MA 02139; and §Department of Biochemistry, College of Medicine, Chung-Ang University, Seoul 156-756, Korea

Contributed by Alexander Rich, July 30, 2004

A conserved feature of poxviruses is a protein, well characterized as E3L in vaccinia virus, that confers IFN resistance on the virus. This protein comprises two domains, an N-terminal Z-DNA-binding protein domain (Zα) and a C-terminal double-stranded RNA-binding domain. Both are required for pathogenicity of vaccinia virus in mice infected by intracranial injection. Here, we describe the crystal structure of the Zα domain from the E3L-like protein of Yaba-like disease virus, a Yatapoxvirus, in a complex with Z-DNA, solved at a 2.0-Å resolution. The DNA contacting surface of Yaba-like disease virus $Z\alpha_{E3L}$ closely resembles that of other structurally defined members of the Zα family, although some variability exists in the β-hairpin region. In contrast to the Z-DNA-contacting surface, the nonbinding surface of members of the Zα family are unrelated; this surface may effect protein-specific interactions. The presence of the conserved and tailored Z-DNA-binding surface, which interacts specifically with the zigzag backbone and *syn* base diagnostic of the Z-form, reinforces the importance to poxvirus infection of the ability of this protein to recognize the Z-conformation.

The Yaba monkey tumor virus (YMTV) and the closely related Yaba-like disease virus (YLDV) are members of the Yatapoxvirus family. Both viruses have double-stranded DNA genomes of ≈150 kilobase pairs and code for >150 proteins (1). YMTV induces histiocytomas with characteristic microscopic morphology in soft tissue of monkeys and baboons (2, 3) and humans (4). YLDV, as well as a third Yatapoxvirus, Tanapox, causes vesicular skin lesions in monkeys and humans (5, 6). Furthermore, YMTV DNA has transforming activity in monkey cell lines (7). The high similarity between the YLDV and YMTV was revealed with the recent sequencing of the Yaba monkey tumor virus (8).

All sequenced poxviruses have a gene, called E3L in vaccinia, that is required for IFN resistance. E3L has been shown to be oncogenic and antiapoptotic; NIH 3T3 cells expressing vaccinia E3L were found to grow faster than control cells, with increased expression of cyclin A and decreased levels of the suppressor molecule p26 (9). When the NIH 3T3 E3L-expressing cells were injected into nude mice, solid tumors were formed. The expression of E3L has been shown to be essential for these oncogenic and antiapoptotic activities.

The E3L protein and its orthologues comprise two domains, an N-terminal Z-DNA-binding protein domain (Zα) and a C-terminal double-stranded RNA-binding domain. A similar Zα motif is found in vertebrate ADAR1 (double-stranded RNA adenosine deaminase) and in the IFN-inducible DLM-1 (also known as ZBP-1) of mammals (10, 11). Extensive biochemical and biophysical studies of human $Z\alpha_{ADAR1}$ show that it binds tightly and specifically to Z-DNA (10, 12–14). Both domains of the mouse-adapted vaccinia virus E3L are essential for pathogenicity in mice (15, 16). The C-terminal domain is sufficient for viral replication in cultured cells *in vitro*. However, both domains are needed to infect and kill mice after an intranasal or intracranial inoculation. The ability to bind Z-DNA is essential for E3L activity; domain swaps with the Zα domains from the human ADAR1 and mouse DLM-1 are equivalent to the wild-type, whereas a replacement of the N-terminal domain of E3L with a domain defective in Z-DNA binding results in a less pathogenic or nonpathogenic virus (16).

The structures of human $Z\alpha_{ADAR1}$ and mouse $Z\alpha_{DLM1}$ have been solved, complexed with Z-DNA (11, 17). These structures show that these proteins, which have limited similarity in amino acid sequences, share closely related DNA-binding interfaces. Recently, the NMR structure of the Zα domain of vaccinia E3L ($vvZ\alpha_{E3L}$), solved in the absence of DNA, showed that this viral Zα domain has a similar topology to other Zα domains (18). The E3L orthologue from YLDV has 39% identity to vaccinia virus E3L, spread throughout both N- and C-terminal domains. Although the sequence identity is <30% when only the Zα motifs are compared, all key DNA-contacting residues are conserved. The Zα motifs of YLDV and YMTV are 70% identical (1, 8), reinforcing the close relationship between these two viruses.

Here, we show that the Zα domain of the E3L orthologue of YLDV ($yabZ\alpha_{E3L}$) binds to Z-DNA tightly and specifically *in vitro*. The crystal structure of a complex between $yabZ\alpha_{E3L}$ and Z-DNA is reported. This structure clearly shows that $yabZ\alpha_{E3L}$ is a member of the Zα family of protein domains. The interactions between $yabZ\alpha_{E3L}$ and Z-DNA are highly conserved with those between $Z\alpha_{ADAR1}$ or $Z\alpha_{DLM1}$ and Z-DNA. Subtle modulations in the interaction surface demonstrate that variations are allowed in this interaction, particularly at the edge of the binding surface. In contrast, the surface facing away from the Z-DNA interface has no resemblance to other Zα domains. This structure demonstrates that viral Zα domains can bind to the Z-conformation in as well engineered a fashion as previously characterized Zα domains from mammalian proteins.

Materials and Methods

Expression and Purification. The gene coding for the Zα domain (residues 2–79) of E3L from YLDV ($yabZ\alpha_{E3L}$) was subcloned into pET28a (Novagen) and transformed into BL21(DE3) (Novagen). The cells were grown in LB containing 30 μg/ml kanamycin to an OD_{600} of 0.7–0.8 at 30°C, and then induced with 0.6 mM isopropyl β-D-thiogalactoside (IPTG) at 18°C for 20 h. $yabZ\alpha_{E3L}$ was purified by using a slight modification of the

Abbreviations: Zα, Z-DNA-binding protein domain; $yabZ\alpha_{E3L}$, Zα domain from the E3L-like protein of Yaba-like disease virus; YMTV, Yaba monkey tumor virus; YLDV, Yaba-like disease virus.

Data deposition: The atomic coordinates have been deposited in the Protein Data Bank, www.pdb.org (PDB ID code 1SFU).

‡To whom correspondence may be addressed. Fax: 617-253-8699 (A.R.). E-mail: kkim@med.skku.ac.kr (K.K.K.) or ygkimmit@cau.ac.kr (Y.-G.K.).

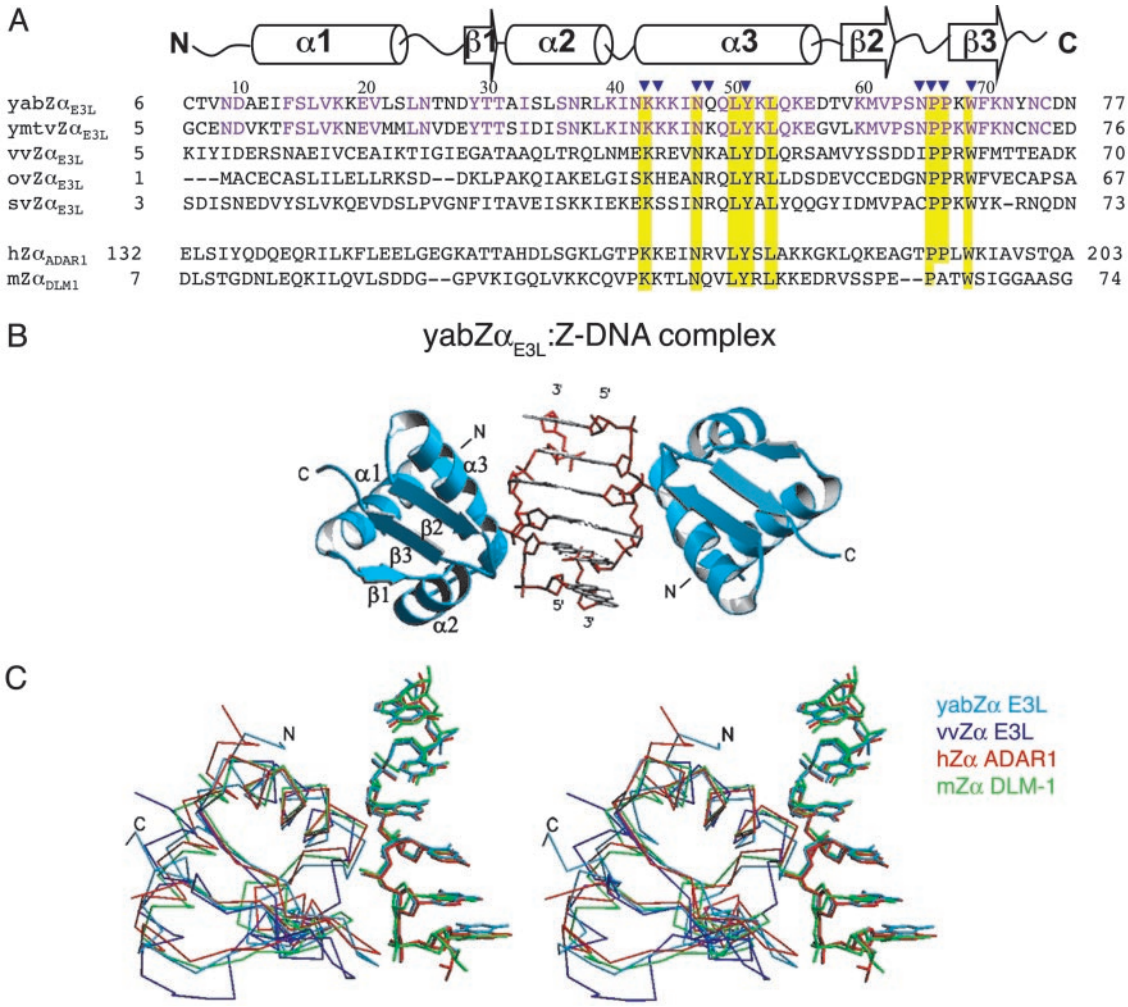

Fig. 1. Sequence and secondary structural comparison of yabZα_{E3L} with the other Z-DNA-binding domains and related poxvirus E3L domains. (*A*) Multiple sequence alignment of the Zα proteins. Numbering and secondary structure elements for the Zα domains of E3L from YLDV (yabZα_{E3L}), YMTV (ymtvZα_{E3L}), vaccinia virus (vvZα_{E3L}), Orf virus (ovZα_{E3L}), and Swinepox virus (svZα_{E3L}), along with human ADAR1 (hZα_{ADAR1}) and mouse DLM1 (mZα_{DLM1}) (accession numbers as in ref. 16, except YMTV NC 005179). Secondary structure is drawn on top of the sequence. The α-helix and β-sheet are represented by tubes and arrows, respectively. The conserved sequences of all Zα family are colored yellow. Residues from yabZα_{E3L} that make contact with the DNA are marked with a blue triangle. (*B*) The overall structure of the yabZα_{E3L}:Z-DNA complex. The N and C terminus and secondary structure elements are labeled. (*C*) Structural superposition of yabZα_{E3L}:Z-DNA (sky blue), hZα_{ADAR1}-Z-DNA (red), mZα_{DLM1}-Z-DNA (green), and vvcZα_{E3L} (royal blue). All DNA atoms and structurally aligned Cα atoms were used for the superposition (64 Cα for hZα_{ADAR1} and 57 Cα for Zα_{DLM}).

method described for purifying hZα_{ADAR1} (17). After a His-affinity column (Amersham Pharmacia Biosciences) and removal of the N-terminal six histidines with thrombin (Boehringer Mannheim), the protein in buffer A (20 mM Hepes, pH 7.5/80 mM NaCl) was further purified by using Resource S (Amersham Pharmacia Biosciences). The purified protein was dialyzed against buffer A and concentrated to 1 mM by using YM-10 ultrafiltration and Centricon (Millipore). All of the steps of buffer exchange were performed by using a PD-10 column (Amersham Pharmacia Biosciences). The protein concentration was measured by using the Bradford method with a BSA standard curve (19).

CD. $(dC\text{-}dG)_6$ (IDT) was rehydrated with a TE buffer (10 mM Tris·Cl, pH 8.0/1 mM EDTA) and annealed before use. The conversion of $(dC\text{-}dG)_6$ from the B- to the Z-conformation was monitored by CD. The CD spectra were obtained at 25°C by using an AVIV model 202. All measurements were carried out by using 50 μg/ml (75 μM base pair) DNA in a CD buffer (10 mM Hepes, pH 7.4/10 mM KF/0.1 mM EDTA) in a 2-mm quartz cell. Protein was added to the DNA solution to a final concentration of 30 μM. The maximum volume of the protein added to the sample did not exceed 5% of the total volume. Spectra for wavelength scanning were recorded at 1-nm intervals, averaged over 3 s. For the kinetic measurements, the CD signal changes at 255 nm were recorded at 0.5-s intervals up to 1 h.

Crystallization and Data Collection. The Zα domain of YLDV and $d(TCGCGCG)_2$ (IDT, Coralville, IA) were purified, mixed and crystallized (S.C.H., D.B.O., Y.-G.K., and K.K.K., unpublished data). Briefly, the protein and DNA in 5 mM Hepes-NaOH (pH 7.5) and 80 mM NaCl were mixed at an equimolar (protein:single strand DNA) ratio, resulting in a final concentration of 0.6 mM each, and incubated at 30°C for at least 10 h. Initial crystallization was performed at 22°C in hanging drops by using Hampton screens I and II and Natrix screen kits, and the vapor diffusion method (Hampton Research, Riverside, CA). The protein–DNA complex (1.5 μl) was mixed with 1.5 μl of a reservoir solution. Orthorhombic crystals were obtained over a reservoir solution containing 25 mM cacodylate-HCl (pH 6.0), 1–1.1 M Li_2SO_4,

and 2–4 mM $MgCl_2$ after 1 month. Br-multiwavelength anomalous dispersion (MAD) x-ray data were collected at the 41XU beam line of the Spring-8 Synchrotron by using a crystal soaked in a solution of 25 mM cacodylate-HCl (pH 6.0), 1 M NaBr, and 25% glycerol for 50 s. All data were processed by using the HKL2000 program (20). Crystals belong to the orthorhombic space group $P2_12_12$, with unit cell constants a = 51.20, b = 92.45, and c = 48.02 Å (Table 1, which is published as supporting information on the PNAS web site).

Structure Determination and Refinement. The Br sites were found, and the initial multiwavelength anomalous dispersion (MAD) phases were calculated and refined by using the programs SOLVE and RESOLVE, respectively (21, 22). The MAD phases were further refined by using solvent flattening, histogram matching, and noncrystallographic symmetry averaging by using the program DM (23). The quality of the final map was sufficient to fit into the model. The model building was performed with the O program (24). The initial model of the protein and DNA was built by locating the Zα and DNA of hADAR1 (chain C and F; PDB code 1QBJ) in a final electron density map. The model was refined with the data set collected at 2.0 Å from the same crystal used for the MAD data collection by using the CNS program (version 1.0) with the MLHL target function The model was then rebuilt against an initial map, a phase combined σA weighted $2F_o - F_c$ map and an $F_o - F_c$ map (25). The stereochemistry of the model was checked with the program PROCHECK at each stage of model building and refinement (26). There were two proteins (chains A and B) and one double-stranded DNA (chains C and D) in the asymmetric unit. Alanine and glycine residues were fitted to disorganized regions with poor electron density (Ala-7, Ala-8, and Ala-9 in chain A; Gly-40 in chain B). The final model included the residues, 6–75 of each protein, 12 nucleotides, and 171 waters (Table 1).

Results and Discussion

Binding of yabZα_{E3L} to Z-DNA. There are nine residues that make specific contacts with Z-DNA in the co-crystal structure of hZα_{ADAR1}:DNA. Eight of these residues are conserved in yabZα_{E3L} (Fig. 1*A*). Therefore, we thought it likely that yabZα_{E3L} would bind to Z-DNA tightly and specifically. This binding was tested by using CD (Fig. 2). The CD spectrum in the range between 240 and 300 nm of Z-DNA is almost a mirror image as compared with that of B-DNA (27). When $(dC\text{-}dG)_6$ is incubated with human Zα_{ADAR1} or mouse Zα_{DLM1}, the spectrum of the DNA rapidly converts to that of Z-DNA (10, 12, 28). In the presence of yabZα_{E3L}, a similar conversion takes place (Fig. 2*A*). The change from B- to Z-DNA over time can be monitored at 255 nm, as shown in Fig. 2*B*. The yabZ$_{E3L}$ domain induces the conversion of B- to Z-DNA as quickly as that of human Zα_{ADAR1}, whereas a somewhat slower conversion was observed with the mouse Zα_{DLM1} (Fig. 2*B*). A comparative study of binding affinities will be presented elsewhere. These spectral results show that the yabZα_{E3L} domain stabilizes the Z-conformation in a manner similar to that seen with the other two domains. Although yabZα_{E3L} and human Zα_{ADAR1} share only 26% sequence identity (Fig. 1*A*), Z-DNA binding by both reinforces the idea that the major factor determining Z-DNA-binding ability mainly resides in the Z-DNA contacting amino acid residues.

Overall Structure of the yabZα_{E3L}–Z-DNA Complex. To further investigate the nature of the interaction between yabZα_{E3L} and DNA, the three-dimensional structure of co-crystals of yabZα_{E3L} and the oligonucleotide, $d(TCGCGCG)_2$ was determined to 2.0 Å with an *R* factor of 23.7% and an R_{free} of 27.0% (Table 1). In the crystal, two yabZα_{E3L} domains are found in the asymmetric unit, each bound to one strand of double-stranded DNA in the Z-conformation (Fig. 1*B*). The proteins do not interact with each other. One Zα domain and its interacting DNA were designated as chains A and C, the other protein–DNA pair were designated as chains B and chain D. The two yabZα_{E3L} domains are related by noncrystallographic symmetry and are nearly identical, with 0.47 Å of rms deviation (rmsd) for 64 Cα atoms. The crystal structure of yabZα_{E3L} clearly verifies that it belongs to the Zα family of helix–turn–helix (HTH), winged-helix Z-DNA-binding proteins. It has an α/β architecture, consisting of three β-strands and three α-helices, as is found in hZα_{ADAR1} and mZα_{DLM1} (Fig. 1*B*). The three α-helices (α1, α2, and α3) form a core domain, which is flanked by a β-sheet of three antiparallel strands (β1, β2, and β3). α2 and α3 form an HTH motif and two antiparallel β-strands (β2 and β3) form the wing.

In the complex, the double-stranded DNA adopts a typical left-handed Z-DNA conformation, with guanine nucleotides in the *syn* conformation and C3′-*endo* sugar puckering except G6, which is in C2′-*endo*. Watson–Crick base pairing is well conserved in this structure. The 5′-dT overhang is not modeled due to its weak electron density.

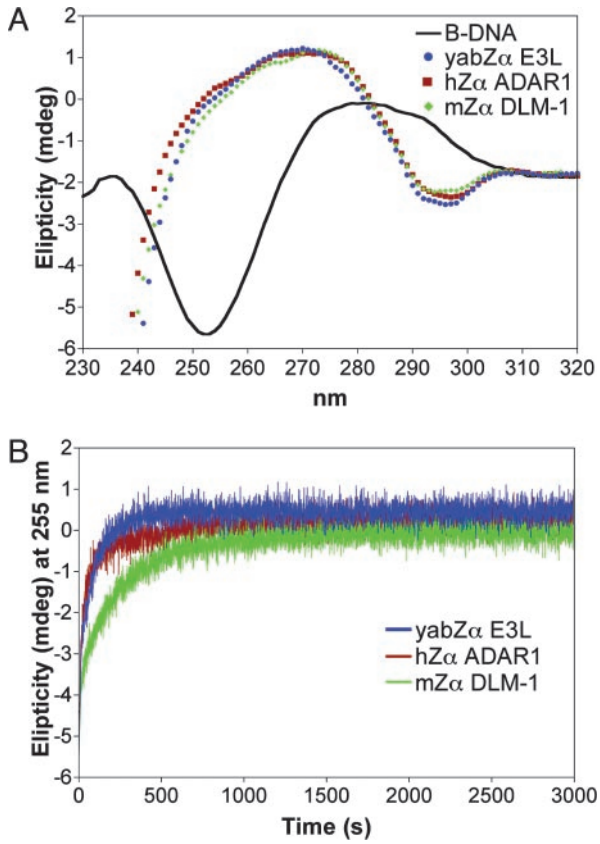

Fig. 2. Interaction of yabZα_{E3L} with Z-DNA. (*A*) Z-DNA binding of yabZα_{E3L} as measured by CD. Unbound $(dC\text{-}dG)_6$ is in the B-form under the buffer conditions used here (green curve). In the presence of a 2.5:1 (base pair:protein) molar ratio of DNA to protein (yabZα_{E3L} in blue, hZα_{ADAR1} in red and mZα_{DLM-1} in green), the DNA adopts the Z-conformation, as shown by the CD spectra. All curves are identical. (*B*) Kinetic measurement of DNA changing from B-DNA to Z-DNA in the presence of yabZα_{E3L}, hZα_{ADAR1}, or mZα_{DLM1}. The change in DNA conformation with time is measured by the change in ellipticity at 255 nm. hZα_{ADAR1} and yabZα_{E3L} show similar kinetics of conversion, whereas mZα_{DLM1} acts slightly more slowly.

Protein–DNA Interaction in yabZα_{E3L}. The interaction between members of the Zα family and Z-DNA is characterized by a single continuous recognition surface involving numerous sugar-phosphate backbone contacts, which provide conformational specificity (11, 17). This recognition surface is made up of residues in the

BIOCHEMISTRY

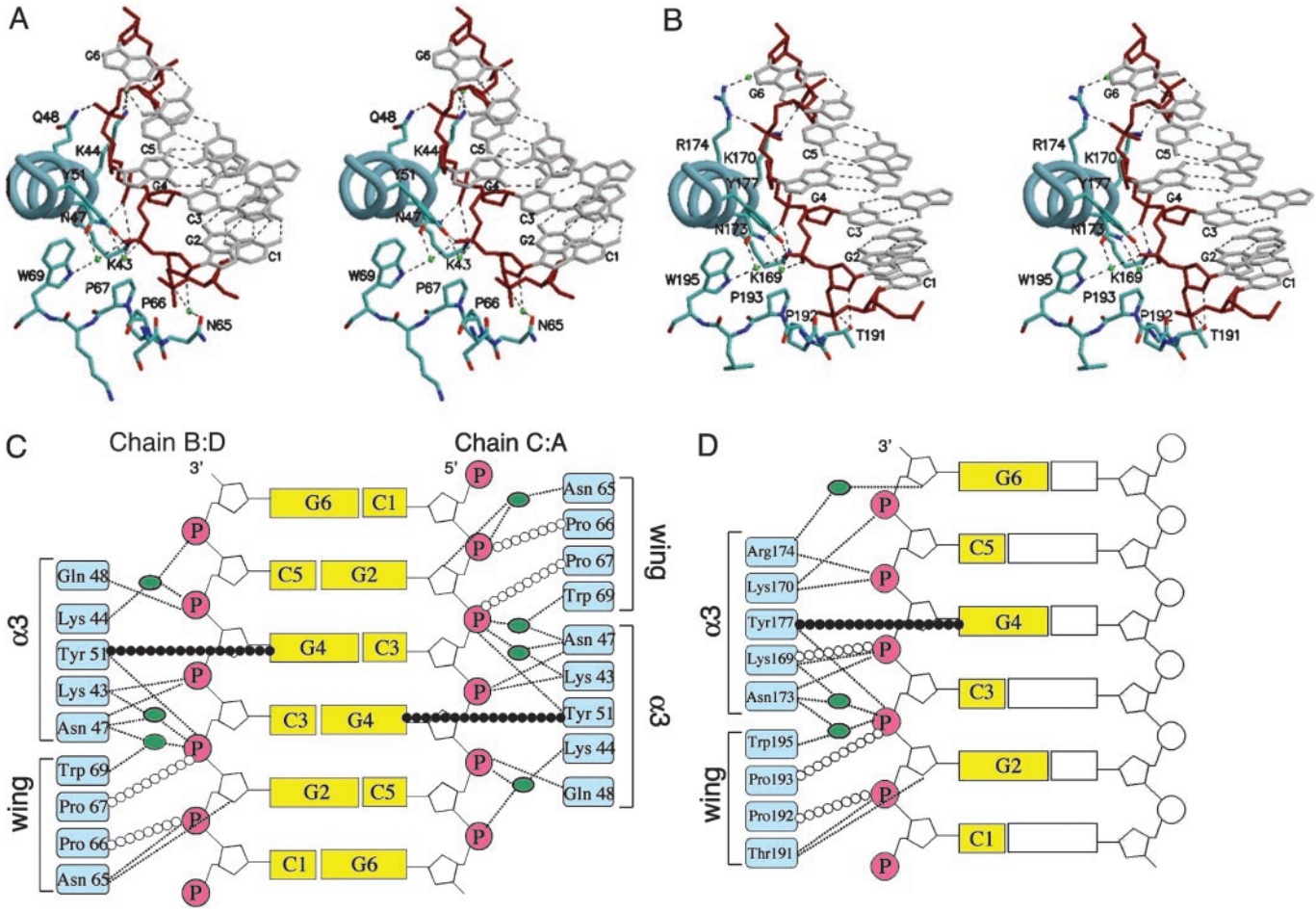

Fig. 3. Comparison of contacts between yabZα_{E3L} or hZα_{ADAR1} with Z-DNA. (*A*) Stereo view of the protein–DNA interface of the yabZα_{E3L}:Z-DNA between chain A and chain C. (*B*) Stereo view of the protein–DNA interface of Zα_{ADAR1}:Z-DNA. Both diagrams are viewed from the C-terminal end of the recognition helix (α3). Water molecules are shown in green. Hydrogen bonds are drawn as dashed lines. The tyrosine on the recognition helix is oriented in an edge-on view. (*C* and *D*) Schematic diagrams of the protein–DNA interactions in the yabZα_{E3L}:Z-DNA (*C*) and hZα_{ADAR1}:Z-DNA (*D*) complexes. Hydrogen bonds are represented by dashed lines and van der Waals contacts by open circles. The CH-π interaction between the conserved Tyr and a *syn*-guanosine is indicated by filled circles. Waters are shown by green ovals.

α3 helix and the "wing." DNA recognition by yabZα_{E3L} has these same properties. Three residues, Asn-47, Tyr-51, and Trp-69 as numbered in yabZα_{E3L} (Asn-173, Tyr-177, and Trp-195 in hZα_{ADAR1}), central to interaction with Z-DNA, are completely conserved within the Zα family (Figs. 1*A* and 3). Asn-47 and Trp-69 make water-mediated hydrogen bonds to the phosphate backbone. Trp-69 also buttresses Tyr-51 by using a distinctive hydrophobic edge-to-face interaction, thereby stabilizing the interaction of Tyr-51 with the C8 of the *syn* guanine G4. In addition to this CH-π interaction, Tyr-51 makes a direct hydrogen bond to a phosphate in the DNA backbone. Glu-48, Lys-43, and Lys-44 from the recognition helix of helix–turn–helix motif also participate in DNA recognition, either directly or through water-mediated hydrogen bonds to the phosphate backbone (Fig. 3).

The importance of the interaction of tyrosine on the recognition helix with DNA has been demonstrated in a biological system assessing vaccinia virus infection of mice. Wild-type virus is lethal for the mouse in intracranial injection. When hZα_{ADAR1} is substituted for vvZα_{E3L}, the chimeric virus retains lethality. However, mutating the recognition helix (Y to F, Y to A) results in significant loss of lethality for both the wild-type and the hZα_{ADAR1} chimeric virus, as well as weaker Z-DNA binding *in vitro* (16). The Tyr-51 of yabZα_{E3L} shows a conformation similar to that found in the hZα_{ADAR1}:Z-DNA complex.

In this crystal, the asymmetric unit contains two yabZα_{E3L} and one double-stranded DNA. Although the contacts between yabZα_{E3L} and each strand of DNA use the same residues and modes, the details of the interactions are slightly different. The most noticeable difference is found in the interaction between the wing hairpin and DNA. In this region, Pro-66, Pro-67, and Asn-65 mediate interactions between Zα and Z-DNA; however, the Asn-65-DNA contact differs between the two forms. In one binding surface (chains B and D), Asn-65 interacts with the phosphate and ribose directly, whereas, in the other side (chains A and C), the hydrogen bonds are water-mediated (Fig. 3). This finding indicates some flexibility in the β-sheet–DNA contacts. The position of the β-turn in the solution structure of vvZα_{E3L} is considerably different from that of the yabZα_{E3L} wing (Fig. 1*C*) (18). It is possible that, in viral proteins, the wing moves as it clasps the Z-DNA and that the two different interactions seen in this crystal are the result of the flexibility that allows this movement. On the other hand, the position and sequence of the wing in mZα_{DLM-1}, which has only one proline in the β turn that contacts Z-DNA, is also different from that of hZα_{ADAR1} and yabZα_{E3L}. The position of the vaccinia wing may be a further example of the variability of this region.

Structural Comparison of yabZα_{E3L}:Z-DNA with other Zα:Z-DNA Complexes. The overall structure of yabZα_{E3L} and its interactions with Z-DNA are very similar with those of hZα_{ADAR1} and mZα_{DLM1}. In

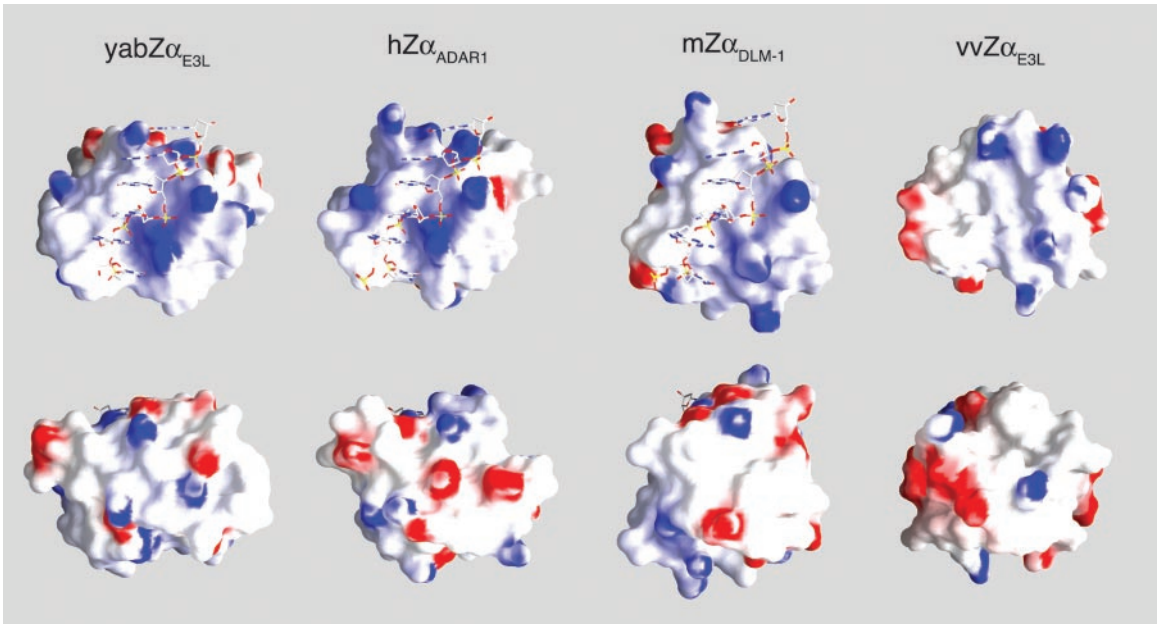

Fig. 4. Surface charge distributions of yabZα_{E3L}, hZα_{ADAR1}, mZα_{DLM1}, and vvZα_{E3L} (from left to right) viewed along the DNA-binding cleft (*Upper*) and rotated 180° on the back side (*Lower*). The red and blue areas represent the negatively and positively charged surfaces, respectively. Skeletal representations showing the bound Z-DNA strand are found in the first three diagrams.

addition, the protein:DNA contacts are similar to those seen in the hZα_{ADAR1}-, mZα_{DLM1}-, and yabZα_{E3L}:Z-DNA structures (18). The hZα_{ADAR1}:Z-DNA complex can be superposed on the yabZα_{E3L}:Z-DNA complex with an rms deviation (rmsd) of 1.10 Å for 64 Cα atoms and six nucleotides, whereas the rmsd between the yabZα_{E3L}:Z-DNA complex and the mZα_{DLM1}:Z-DNA complex is 1.37 Å when 57 Cα atoms and six nucleotides were used for calculation. Therefore, yabZα_{E3L} is more similar to hZα_{ADAR1} than to mZα_{DLM1}. The most prominent differences between these structures are seen in the wing (β2 and β3). mZα_{DLM1} has a shorter wing, which is positioned closer to the α3 helix, whereas the wings of yabZα_{E3L} and hZα_{ADAR1} in complex with Z-DNA are nearly identical (Fig. 1*C*). It is possible that the slower B- to Z-conversion rate observed for mZα_{DLM1} is be related to the different shape of the wing (Figs. 1*C* and 2*B*).

In vvZα_{E3L}, the solution structure shows that Tyr 48, orthologous to Tyr-51 of yabZα_{E3L}, adopts a different side chain conformation in the absence of Z-DNA. However, when vvZα_{E3L} is bound to DNA, the tyrosine adopts a configuration similar to that seen in hZα_{ADAR1}, suggesting that the Z-DNA contacting surface of vvZα_{E3L} is very similar when the protein is bound to Z-DNA. The requirement for a change in conformation of the protein upon binding may result in the slower binding kinetics of vvZα_{E3L} as compared with other Zα domains.

When bound to DNA, a surface area of 744 Å^2 is buried in yabZα_{E3L}, comparable with 725 Å^2 for hZα_{ADAR1} and 740 Å^2 for mZα_{DLM1} (11), which suggests that these three Zα proteins should have similar binding affinities for Z-DNA.

The Z-DNA-binding surfaces of the four Zα domains whose three-dimensional structure has been determined show very similar curvature and charge distribution (Fig. 4 *Upper*), making a tailored fit for the ligand. The first three (yabZα_{E3L}, hZα_{ADAR1}, mZα_{DLM1}) were solved bound to Z-DNA, and the bound strand is shown on the surface. The fourth protein, vvZα_{E3L}, was solved in solution without Z-DNA. Analysis of its interactions with Z-DNA shows that the DNA occupies the same position as in the first three diagrams. In each case, the central binding surface is lined with positive charges, especially around the periphery of the binding site. A white "bulge" in the center of the first three figures represents the tyrosine on the recognition helix whose face interacts with a *syn* guanine residue. That bulge is missing in the vvZα_{E3L}, because the tyrosine has rotated to the top of the binding surface. The position of this tyrosine is variable in solution; Fig. 4 shows the predominant position, in which the tyrosine prevents binding to Z-DNA. Binding to Z-DNA requires the tyrosine to rotate down into the center of the binding surface.

It is interesting that the distribution of positive charges around the binding site in the top row varies somewhat in all four structures. Fig. 4 *Lower* shows the nonbinding "back" side of the Zα domains, on which an apparently random distribution of positive and negative charges is seen. This result is not surprising because these proteins are likely to have other functions in addition to Z-DNA binding, even though many of these functions are not known at present.

Conclusion

In this paper, we have described the interactions of the Zα domain of the E3L-like protein of YLDV with DNA by using spectroscopic and crystallographic studies. This E3L-like protein is known to play a key role in poxvirus pathogenesis, as is best documented in vaccinia virus infections. The yabZα_{E3L} readily converts B-DNA to Z-DNA and is comparable in activity to Zα domains from hADAR1 and mDLM1 (Fig. 2*C*). The overall structure of yabZα_{E3L} and its Z-DNA recognition in the complex are extremely similar to those of the mZα_{DLM1}:Z-DNA and hZα_{ADAR}:Z-DNA complexes, because yabZα_{E3L} also uses a winged helix–turn–helix motif to recognize the zigzag backbone and *syn* base of Z-DNA. The critical and conserved residues of yabZα_{E3L} for Z-DNA recognition also have similar interactions for Z-DNA recognition at the same position. In addition, a few different structural features found among the Zα domains might be related to their different roles in Z-DNA binding and related functions in the cell.

The presence of a protein, precisely tailored to fit Z-DNA, supports the importance in poxviruses of binding to this unusual conformation. Although yabZα_{E3L} resembles previously studied Zα domains in every way, it is also important to notice the differences between these domains, which may be related to specific function.

This work was supported by Korea Research Foundation Grant KRF-2003-015-E00058 (to K.K.K.), a National Institutes of Health grant, and grants from the Dana and Ellison Medical Foundations (to A.R.). The synchrotron radiation experiments were carried out at Spring-8 in cooperation with the Japan Synchrotron Radiation Research Institute (JASRI) (proposal no. 2002B0055-NL1-np).

1. Lee, H. J., Essani, K. & Smith, G. L. (2001) *Virology* **281,** 170–192.
2. Whittaker, D. & Glaister, J. R. (1985) *Lab. Anim.* **19,** 177–179.
3. Schielke, J. E., Kalishman, J., Liggitt, D. & Bielefeldt-Ohmann, H. (2002) *Contemp. Top. Lab. Anim. Sci.* **41,** 27–29.
4. Rouhandeh, H., Vafai, A. & Kilpatrick, D. (1984) *J. Ultrastruct. Res.* **86,** 100–105.
5. Knight, J. C., Novembre, F. J., Brown, D. R., Goldsmith, C. S. & Esposito, J. J. (1989) *Virology* **172,** 116–124.
6. McNulty, W. P., Jr., Lobitz, W. C., Jr., Hu, F., Maruffo, C. A. & Hall, A. S. (1968) *Arch. Dermatol.* **97,** 286–293.
7. Rouhandeh, H. & Vafai, A. (1982) *Virology* **120,** 77–92.
8. Brunetti, C. R., Amano, H., Ueda, Y., Qin, J., Miyamura, T., Suzuki, T., Li, X., Barrett, J. W. & McFadden, G. (2003) *J. Virol.* **77,** 13335–13347.
9. Garcia, M. A., Guerra, S., Gil, J., Jimenez, V. & Esteban, M. (2002) *Oncogene* **21,** 8379–8387.
10. Herbert, A., Alfken, J., Kim, Y. G., Mian, I. S., Nishikura, K. & Rich, A. (1997) *Proc. Natl. Acad. Sci. USA* **94,** 8421–8426.
11. Schwartz, T., Behlke, J., Lowenhaupt, K., Heinemann, U. & Rich, A. (2001) *Nat. Struct. Biol.* **8,** 761–765.
12. Berger, I., Winston, W., Manoharan, R., Schwartz, T., Alfken, J., Kim, Y. G., Lowenhaupt, K., Herbert, A. & Rich, A. (1998) *Biochemistry* **37,** 13313–13321.
13. Kim, Y. G., Lowenhaupt, K., Schwartz, T. & Rich, A. (1999) *J. Biol. Chem.* **274,** 19081–19086.
14. Kim, Y. G., Lowenhaupt, K., Maas, S., Herbert, A., Schwartz, T. & Rich, A. (2000) *J. Biol. Chem.* **275,** 26828–26833.
15. Brandt, T. A. & Jacobs, B. L. (2001) *J. Virol.* **75,** 850–856.
16. Kim, Y. G., Muralinath, M., Brandt, T., Pearcy, M., Hauns, K., Lowenhaupt, K., Jacobs, B. L. & Rich, A. (2003) *Proc. Natl. Acad. Sci. USA* **100,** 6974–6979.
17. Schwartz, T., Rould, M. A., Lowenhaupt, K., Herbert, A. & Rich, A. (1999) *Science* **284,** 1841–1845.
18. Kahmann, J. D., Wecking, D. A., Putter, V., Lowenhaupt, K., Kim, Y. G., Schmieder, P., Oschkinat, H., Rich, A. & Schade, M. (2004) *Proc. Natl. Acad. Sci. USA* **101,** 2712–2717.
19. Bradford, M. M. (1976) *Anal. Biochem.* **72,** 248–254.
20. Otwinowski, Z. & Minor, W. (1997) *Methods Enzymol.* **276,** 307–326.
21. Terwilliger, T. C. & Berendzen, J. (1999) *Acta Crystallogr. D Biol. Crystallogr.* **55,** 849–861.
22. Terwilliger, T. C. (2001) *Acta Crystallogr. D Biol. Crystallogr.* **57,** 1763–1775.
23. Cowtan, K. D. & Zhang, K. Y. (1999) *Prog. Biophys. Mol. Biol.* **72,** 245–270.
24. Jones, T. A., Zou, J. Y., Cowan, S. W. & Kjeldgaard. (1991) *Acta Crystallogr. A* **47,** 110–119.
25. Brunger, A. T., Adams, P. D., Clore, G. M., DeLano, W. L., Gros, P., Grosse-Kunstleve, R. W., Jiang, J. S., Kuszewski, J., Nilges, M., Pannu, N. S., *et al.* (1998) *Acta Crystallogr. D Biol. Crystallogr.* **54,** 905–921.
26. Laskowski, R. A., MacArthur, M. W., Moss, D. S. & Thornton, J. M. (1993) *J. Appl. Crystallogr.* **26,** 283–291.
27. Pohl, F. M. & Jovin, T. M. (1972) *J. Mol. Biol.* **67,** 375–396.
28. Herbert, A., Schade, M., Lowenhaupt, K., Alfken, J., Schwartz, T., Shlyakhtenko, L. S., Lyubchenko, Y. L. & Rich, A. (1998) *Nucleic Acids Res.* **26,** 3486–3493.